IJRCS

International Journal of Robotics and Control Systems
Vol. 5, No. 1, 2025, pp. 479-499
ISSN 2775-2658
http://pubs2.ascee.org/index.php/ijrcs

ASCEE

Two-Flexible-Link Manipulator Vibration Reduction Through Fuzzy-Based Position

Waleed F. Faris [a,b], M. Rabie [c], Ahmad O. Moaaz [d], Nouby M. Ghazaly [e,f,1,*], Mostafa M. Makrahy [c]

[a] Department of Mechanical Engineering, International Islamic University Malaysia, Kuala Lumpur, Malaysia
[b] Visiting Professor, University Nevada Las Vegas, United States
[c] Automotive and Tractor Eng. Dept., College of Engineering, Minia University, 61519, El-Minia, Egypt
[d] Mechanical Engineering Department, Faculty of Engineering, Beni-Suef University, 62521, Beni-Suef, Egypt
[e] Technical College, Imam Ja'afar Al-Sadiq University, Baghdad, Iraq
[f] Department of Mechanical Engineering, South Valley University, Qena, Egypt
[1] noby_mehdi@ijsu.edu.iq
* Corresponding Author

ARTICLE INFO

Article history
Received October 10, 2024
Revised November 30, 2024
Accepted January 17, 2025

Keywords
Robot;
Manipulator;
Fuzzy Logic Controller (FLC);
Linear Quadratic Controller (LQR);
Qaunser Robot

ABSTRACT

The increasing demand for robotic applications has emphasized the need for advanced control strategies, particularly for flexible manipulators with lightweight links. These manipulators offer advantages such as reduced energy consumption, increased payload capacity, and precise high-speed operation but face challenges due to oscillations and delays caused by their flexibility. This study evaluates the performance of Fuzzy Logic Control (FLC) and Linear Quadratic Regulator (LQR) techniques for a Quanser two-link flexible manipulator, using quantitative metrics to compare their effectiveness. The LQR controller was implemented using state-space modeling, with weighting matrices Q and R tuned to achieve minimal overshoot and fast settling times. The FLC system employed five triangular membership functions for inputs and outputs, covering normalized ranges of [-1, 1] for angular errors and [-2.75, 2.75] for error rates, with a heuristic rule base designed to optimize performance. Simulations were conducted under step input conditions at target angles of 30° and 60°, with performance evaluated using vibration amplitude, settling time, steady-state error, and overshoot. Quantitatively, the LQR controller reduced vibration amplitudes to 5 radians for a 30° input and achieved settling times of approximately 2 seconds. For the same conditions, the FLC system reduced vibrations further to 4 radians, though with slightly longer settling times of around 2.3 seconds. At a 60° input, LQR vibrations peaked at over 10 radians, while FLC maintained peak vibrations at approximately 4 radians. These results highlight the FLC's superior vibration suppression, particularly at higher input angles, albeit with marginally slower response times. However, the study was limited to idealized simulation conditions and requires further experimental validation. This research underscores the trade-offs between LQR's precision and FLC's adaptability, emphasizing the importance of parameter tuning and system modeling in achieving optimal performance for flexible manipulators.

1. Introduction

Flexible manipulators, equipped with lightweight, flexible links, are increasingly employed in applications requiring high payload capacity, extended reach, and energy efficiency, such as in aerospace, medical robotics, and high-precision manufacturing. However, their flexibility introduces challenges, including oscillations and delays, that can negatively impact system performance, especially in high-speed, precise tasks. These issues arise from the complex nonlinear dynamics of flexible structures, making effective control critical for ensuring stability and accuracy. To address these challenges, advanced control strategies are needed to reduce oscillations and delay times while maintaining precise control over the manipulator's movement. While traditional control methods like PID controllers have been commonly used, they often fail to manage the nonlinearities and dynamic uncertainties associated with flexible manipulators. This has led to the exploration of alternative control techniques, such as Fuzzy Logic Control (FLC) and Linear Quadratic Regulator (LQR), which offer potential advantages in improving system performance. This study focuses on comparing the effectiveness of FLC and LQR for controlling a Quanser two-link flexible manipulator. The aim is to evaluate and contrast the two methods in terms of their ability to minimize oscillations, reduce delay times, and enhance system response. While LQR is well-established for handling linear systems and optimizing control effort, FLC offers greater adaptability by incorporating heuristic, rule-based decision-making to manage nonlinearities and uncertainties.

The necessity of robotic applications has increased recently, which has made it even more important to look at a variety of robot-related scenarios. It's becoming common practice to use flexible manipulators to save weight and boost payload carrying capability. Because flexible manipulators use extensive links, their lightweight connections improve the manipulator's reachability, increase its payload, and lower the energy required to run the manipulator. Furthermore, flexible manipulators are becoming increasingly and more interesting due to the increased necessity for accurate high-speed operation [1].

Mechanisms of this type are essential for space structure applications, where large, lightweight robots will be employed for various tasks like as space station upkeep, spacecraft repair, and deployment. Flexibility is not a feature of the mechanism; rather, it is an undesirable byproduct that results from balancing mass and length limits to maximize the robot's efficacy. These requirements and constraints on mass and rigidity give rise to a number of interesting control-related issues.

A great deal of research has been done on flexible manipulators, especially in the fields of modeling, vibration control, inverse kinematics, and inverse dynamics. The oscillating reaction that persists for some time after the motion is completed [2] severely limits the flexible manipulators' performance and causes a delay in any subsequent operations. The main objective is to decrease oscillations and delay time. Several control strategies, such as feed-forward control, self-tuning control, modal reference adaptive control, and conventional PID control, are used to control the motion of the manipulators [3]. For each of these strategies, an accurate and efficient mathematical model is needed.

Several control schemes are used with flexible robots, including algebraic control, optimal and robust control, and input shaping control, boundary control, lead-lag control, sliding mode control, adaptive control, neural network-based control, proportional derivative control, and stable inversion in the frequency and time domains. Control strategies for flexible manipulator systems can be classified as either feed-forward (open loop) or feedback (closed loop). Feed-forward techniques for vibration suppression create the control input while considering the physical and vibration properties of the system in order to reduce vibrations during response modes. This approach did not require any additional sensors or actuators and did not take system changes into account once the input was generated. On the other hand, feedback control techniques reduce vibration through the estimation and measurement of system states.

It has been observed that joint trajectory tracking, end-effector trajectory tracking, end-effector regulation challenges, and end-effector to-rest motion in a desired fixed time were the main control objectives for flexible manipulators. Because the system dynamics are not at a minimal phase,

the last one was the most demanding [5]. Because of this, even in cases when a reasonably realistic model of the flexible robot can be produced, it is sometimes too complex to implement during the controller creation process, especially for many control design methodologies that require the plant to make strict assumptions (such linearity) [6].

A cloud model-based controller for tip vibration reduction and trajectory tracking on a flexible-link manipulator was developed. The feasibility, robustness, and effectiveness of the proposed control technique were verified using a flexible-link manipulator test bed. The results of the experiments showed that the controller could take into account the dynamic uncertainty irrespective of the properties of the robot model, and that the cloud theory provides a simple and effective way to implement the fuzziness and randomness found in the language control rules. Stability was demonstrated using a gain-adaptive Direct Strain Feedback (DSFB) control [7]. While gain-fixed DSFB control guarantees closed-loop stability at all times, variations in the robot arm's tip load can lead to suboptimal control performance. Luo and Shwa proposed a simple gain adaptive technique to overcome this issue. The closed-loop stability of gain adaptive DSFB control was established theoretically, and several experiments confirmed the effectiveness of the proposed control scheme. To demonstrate the effectiveness of gain adaptive DSFB control, they examined control performances under variations in the arm's tip load for both the case of adaptive feedback gain and the case of fixed constant feedback gain. The modified gain adaptive law of integration type was utilized [8].

For flexible manipulators, Morris and Madani have proposed a hybrid position/force control technique based on the force-elasticity deflection relationship. They compared computed torque control with quadratic optimal control. The closed-loop, quadratic optimal controller performed significantly better than computed torque control, which was essentially an open-loop technique. However, it might have reduced the size and length of link oscillations to some amount. The experimental results showed that the system responses agreed well with the simulated results. Examining these results, one may conclude that the control mechanism was effective under specific assumptions [9].

Even if the controller did not guarantee the global stability of the starting system, the experimental results showed the applicability of the proposed model and feedback control rule. Even with a few small early tracking issues, the recommended controller operated flawlessly. Experimental results showed that the vibration of the flexible connections was stimulated and the controller could not maintain global stability when there were large initial tracking errors and the planned tip speed was too fast [10].

After examining the challenges with the controllers of the classic flexible manipulators, a dynamic trajectory controller for the 2 DOF flexible manipulator was designed with internal stabilization taken into account. It was shown that the macro-micro system might be used to overcome the problems, and a new controller that made use of this method was suggested. The effectiveness of the macro-micro system for flexible manipulator trajectory control was shown by the modeling and experiment findings [11]. A vertical planar manipulator was used to demonstrate and test a controller with impulse force moment for a two-link flexible manipulator. The flexible manipulator was detached from the two-link manipulators' elastic vibrations. This technology's most important contribution was to simplify controller design, which allowed impulse force moment to easily regulate elastic vibration. Joint trajectory tracking control was shown to be asymptotically stable, and this was made possible by applying the Lyapunov function. According to the simulation results, this approach can accurately follow the tip trajectory of the manipulator [12].

Position control and vibration were achieved using a range of technologies. In [14]-[17], PID fuzzy logic, shape memory alloy, and other hybrid approaches are examined and applied. A study has been conducted on the hybrid position/force control of limited flexible manipulators. To account for greater uncertainty and approximate manipulator dynamics, a novel control law based on RNNs was introduced. We looked into convergence and local stability. A composite controller was built using the suggested control law. When physical traits and outside factors changed, the ability to adapt was put to the test. Additionally, external uncertainties were taken into account, such as errors in the initial

position. The recommended neural network methodology performed better than the PID method, according to the simulation results [13].

The concepts and process of neural network control for flexible-link manipulators using rigid models were introduced. Perturbation control, which stabilized the flexible arm and strengthened its resilience in the face of system uncertainties or disturbances, was provided by the neural network identification and control. Using the stiff model for identifying the forward dynamics of the flexible manipulator in conjunction with the error back-propagation of another neural network (FNN A), a method for learning the connection weights of the neural network (FNN B) for control was devised. An unknown nonlinear plant is not used in the suggested neural control technique for flexible limbs to propagate errors backward.

A computer-simulated planar two-link flexible arm was tested. The robustness of the control system in the event that the payload was altered was examined through extensive simulations. The outcomes of the simulation demonstrated that the suggested control rule had good trajectory tracking and active damping performance. Nevertheless, the robustness of the back-propagation method with respect to variations in payload was restricted by its ability to adapt online. Further research is necessary for realistic implementations of the suggested rigid model-based neural identification control approach, as evidenced by laboratory experiments and improved network architectures [18]. The highly oscillating nature of the vibration modes and the challenges of gathering precise state data guaranteed the stability and effectiveness of nonlinear control laws in both non-adaptive and adaptive schemes [19].

A nonlinear control rule was offered in both nonadaptive and adaptive forms for flexible manipulator motion control. By using the well-known Lyapunov theory, the asymptotic stability of the closed-loop system was guaranteed. Tests with a dual-link flexible arm validated the effectiveness of the suggested systems. Nevertheless, when the motor is running, there is some extremely oscillatory behavior of the vibration modes. This is due to the inability to obtain accurate state measurements and/or the high-frequency external noise from the air-injection system. We employed a first-order digital filter in the state measurement computation and a second-order analog filter in the strain gauge amplifier to mitigate the observation spillover problem. To guarantee the internal stability of the closed-loop system, the cutoff frequencies of these filters were carefully chosen [7].

A technique for manipulating position in a flexible manipulator with several degrees of freedom was developed by Matsuno, Tanaka, and Masao Ikeda. The proposed method regulates the workspace location by giving feedback on the displacement and reaction torque caused by the arm's elastic deformation. The displacement feedback allowed for a rapid motion response, while the reaction torque feedback increased system stability. Robustness and stability of the controller were generally traded off. By including deflection feedback in the workspace and reaction torque feedback in the joint space, the suggested method significantly improved stability and robustness. That was among the standout features of the suggested strategy.

The results of the studies demonstrated the value of the suggested approach for manipulating the flexible manipulator with many degrees of freedom in the workspace [19].

A practical approach to vibration suppression control in flexible robots is presented in this research study. The gravitational effect and the nonlinearity of the actuators were made simple to handle by the use of velocity servo cards. A vibration suppression word can be added to the command used in stiff robots to calculate a velocity instruction. Pseudo-inverse non-linear decoupling (PND) or optimum quadratic control theory (OQC) can be used to determine this term. Using LQR and fuzzy logic control techniques, an intelligent controller is developed to lessen vibration at the link's tip. The experimental setup and findings are presented together with a comprehensive explanation.

The problem statement of this research is to identify the most effective control strategy for minimizing oscillations and reducing delay times in a Quanser two-link flexible manipulator. Specifically, this study aims to compare the performance of FLC and LQR controllers in addressing these issues. The goal is to determine which of these two control methods provides the best trade-off

between vibration suppression and system response time under realistic operational conditions. To evaluate the effectiveness of each controller, quantitative metrics such as vibration amplitude, settling time, and steady-state error will be used. This research will contribute to the development of more robust control strategies for flexible manipulators, ensuring improved precision and reliability in applications that require fast and accurate motion control.

Research Questions

1. How do Fuzzy Logic Control (FLC) and Linear Quadratic Regulator (LQR) compare in terms of vibration suppression for a two-link flexible manipulator?
2. Which control strategy, FLC or LQR, is more effective at reducing delay times in the system's response?
3. What are the trade-offs between FLC's adaptability to nonlinearities and LQR's precision in minimizing control effort and improving system performance?
4. How do different input conditions (e.g., angles of 30° and 60°) affect the performance of FLC and LQR in terms of settling time, vibration amplitude, and steady-state error?

Hypotheses

1. The FLC system will outperform the LQR controller in reducing vibration amplitudes, especially under conditions of high nonlinearity and uncertainty.
2. The LQR controller will exhibit faster settling times and more accurate control at lower input angles (e.g., 30°) compared to the FLC system.
3. FLC will demonstrate greater adaptability to varying conditions and system disturbances, while LQR will provide a more consistent, optimal response under well-defined conditions.

2. Methodology

This research uses simulation-based experiments to compare the performance of FLC and LQR controllers in controlling the flexible manipulator. The LQR technique is applied using state-space modeling and optimal control principles, with tuning of the weighting matrices QQQ and RRR to balance control effort and system performance. The FLC system is designed with five triangular membership functions for both input and output variables, covering ranges from [-1, 1] for angular errors and [-2.75, 2.75] for error rates. A rule-based decision structure is developed to adapt the control action based on the system's state, allowing for better handling of nonlinearities and uncertainties. Simulations are conducted under step input conditions at target angles of 30° and 60°, and the performance of both controllers is assessed based on vibration suppression, settling time, and steady-state error. This methodology allows for a direct comparison of the two control strategies under controlled conditions, highlighting their strengths and weaknesses in addressing the unique challenges posed by flexible manipulators.

The significance of this research lies in its ability to provide a comparative analysis of two advanced control strategies—FLC and LQR—specifically tailored for flexible manipulators. By examining these techniques through simulation, the study offers insights into their respective advantages in minimizing oscillations and delays, which are critical factors for improving the precision and reliability of flexible robotic systems. The findings of this research could inform the design of more efficient and adaptable control systems for a range of real-world applications, from space exploration to high-precision manufacturing.

3. Experimental Setup

The experimental setup consists of a Quanser two-link flexible manipulator, which includes two flexible links driven by DC motors and equipped with sensors to measure their motion and vibrations. The manipulator operates in a horizontal plane, and the configuration is as follows:

- Motors: The system includes two DC motors, one for the shoulder link and another for the elbow link. Both motors are equipped with quadrature optical encoders to measure the angular positions of the joints.
- Sensors: The manipulator is fitted with two accelerometers at the endpoints of the links to measure the accelerations at these locations. Additionally, strain gauges are placed at the clamped ends of both flexible links to monitor the strain and calculate the deflection and vibration of the links.
    - Strain Gauges: Each link is equipped with a strain gauge located at the clamped end. These strain gauges measure the strain caused by the deformation of the link under load, which is used to estimate the displacement and vibrations at the link's tip.
    - Accelerometers: Two accelerometers are positioned at the tip of each link to detect the accelerations caused by the oscillations. These sensors provide real-time data that allows for accurate monitoring of the link movements.
- Control Interface: The system is connected to a computer-based interface that communicates with the sensors and motors, allowing for real-time data collection and control signal adjustments during experiments.

The manipulator is controlled using either FLC or LQR, and performance is evaluated based on the reduction in vibration amplitude, settling time, and steady-state error.

The two primary components of Quanser's [18] two-link flexible robot, which is seen in Fig. 1, are the robot and its sensors, and the computer and robot interface. The two flexible links that make up the robot are limited to working in the horizontal plane. A counterbalanced aluminum strip known as the "shoulder link" is powered by a DC direct-drive motor with an input voltage of v1. A smaller metal strip called the "elbow link" is fixed to the shoulder link terminal. With an input voltage of v2, the elbow link actuator is a geared DC motor. Two accelerometers installed on the link endpoints to detect the accelerations a1 and a2, as well as two optical encoders for the motor shaft locations Θ1 and Θ2, make up the robot's sensors. Robotic endpoint position monitoring is done with strain gauges.

Fig. 1 shows the 2-Degree-Of-Freedom (DOF) Serial Flexible Link (2DSFL) Robot. This robot system is made up of two DC motors that are connected to a two-bar serial linkage via harmonic gearboxes with zero backlash. Both links have strain gauges installed and are flexible. The second harmonic drive (shoulder), to which another flexible link is coupled, is carried at the end of the primary link, which is firmly clamped to the first drive (elbow). Quadrature optical encoders are used as instrumentation for both motors. One strain gauge sensor, which is situated at the clamped end of each flexible link, is included with each link. The mechanical systems that include robot arms typically have features like tensional compliance and serial linkage flexibility, which the robotic mechanism that is being described mimics. Furthermore, the control issues with this system are akin to those in big light-space structures, where flexible structures need to be managed by feedback mechanisms due to weight limits.

3.1. System Modeling

The state space equations of the system to be managed are represented by the state space variables, which are computed using Maple. These are as follows:

$$A = \begin{bmatrix} 0 & 0 & 1 & 0 \\ 0 & 2012 & -91.4 & 1 \\ 0 & -2141 & 91.4 & 0 \\ 0 & 0 & 0 & 5 \end{bmatrix}, B = \begin{bmatrix} 0 \\ 0 \\ 816.6 \\ -816.6 \end{bmatrix}, c = \begin{bmatrix} 1 & 0 \\ 0 & 1 \end{bmatrix}, D = \begin{bmatrix} 0 \\ 0 \end{bmatrix}$$

They suggest that there are two inputs and two outputs in the system. The tip deflection (αn), which represents the displacement of the link at its tip, and theta (Δn), which represents the required angle of the moving link, are the two inputs. The corrected tip deflection and corrected theta are the modeling equation's outputs.

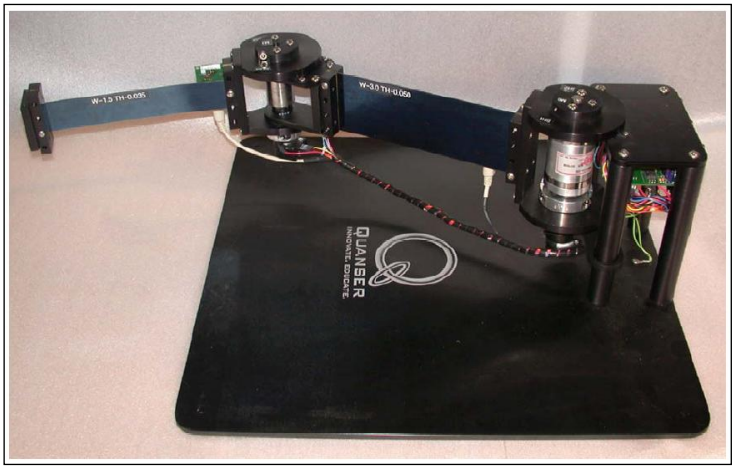

Fig. 1. Quanser two-link flexible robot [3]

The base strain of any flexible link is determined at the clamped end of the link and can be represented using the following formula:

$$E_b = \frac{6F\ L_b}{M_e\ X\ T^2} \tag{1}$$

where F is the load force applied at the link's tip, Lb is the distance from the load (i.e., link tip) to the strain gauge sensor on the clamped end of the link, and X, T, and Me are the flexible link width, thickness, and modulus of elasticity for steel.

The deflection of the beam tip from its base strain gauge (at its clamped end) for a particular beam geometry and material is dependent on the load applied F and the position along the beam length Lb. The expression for the deflection of the link tip, Y, is as follows:

$$Y = \frac{4\ F\ {L_b}^3}{M_e\ X\ T^3} \tag{2}$$

It is also possible to represent the link deflection at the tip, Y, as a function of the link base strain, or the strain at the link base gauge location, in the following way:

$$Y = \frac{2}{3}\ \frac{E_b\ {L_b}^2}{T} \tag{3}$$

As a result, the flexible link tip Kl's equivalent linear stiffness can be written as,

$$K_l = \left(\frac{F}{Y} = \frac{1}{4}\ \frac{M_e\ X\ T^3}{{L_b}^3}\right) \tag{4}$$

The flexible link tip Kr resulting equivalent rotational stiffness can be written as follows:

$$K_r = K_l\ {L_b}^2 = \frac{1}{4}\ \frac{M_e\ X\ T^3}{L_b} \tag{5}$$

3.2. LQR Control

The task at hand involves creating a control system that will quickly and with the least amount of vibrations place the robot tip in a plane (2-DOF). The two-bar serial kinematic mechanism with two flexible links tracks and/or regulates the end-effector planar position. A decoupled state-feedback control is provided to the Multi-Input Multi-Output (MIMO) system, which minimizes link-coupling effects and oscillations produced by flexibility. One pair of flexible links is supplied to the

Two-Degree-Of-Freedom Serial Flexible Link robot. This pair consists of a three-inch-wide steel beam and a one-and-a-half-inch-wide beam. Every beam differs in thickness, or stiffness. Table 1 provides the dimensions of the flexible link.

Table 1. Flexible steel beam dimensions

	Description	Value in (mm)
Steel Beam 1	Width	76.2
	Thickness	1.27
	Free Length	22
Steel Beam 2	Width	38.1
	Thickness	0.89
	Free Length	22

Fig. 2 shows a schematic of the Two-Degree-Of-Freedom Serial Flexible Link (2DSFL) system. It shows the two movable joints that are driven by separate drive systems and linked in series.

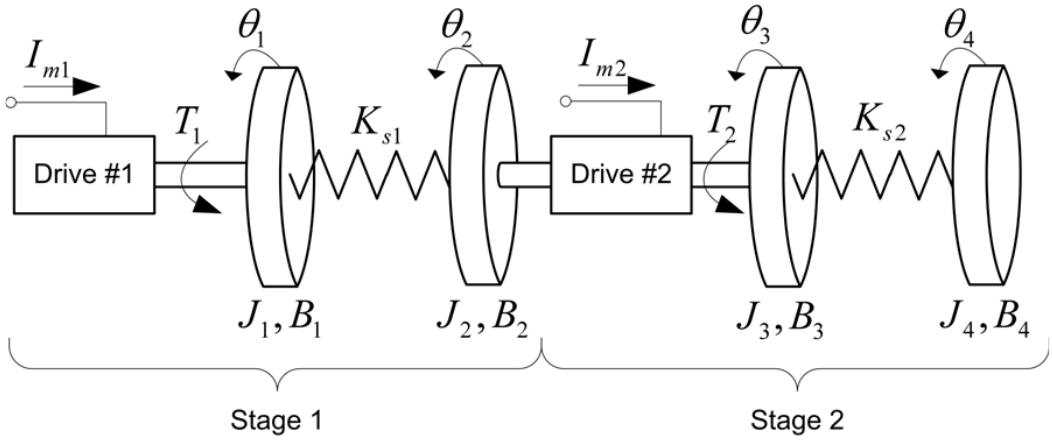

Fig. 2. Schematic of the two-degree-of-freedom serial flexible link system

As shown in Fig. 2, the 2DSFL system is seen as decoupled and divided into two distinct and independent stages: Stage 1 and Stage 2. This is the controller design process that will be outlined below. Each stage has its own LQR state-feedback control loop. Considering the 2DSFL plant's first stage system, Fig. 3 shows its schematic.

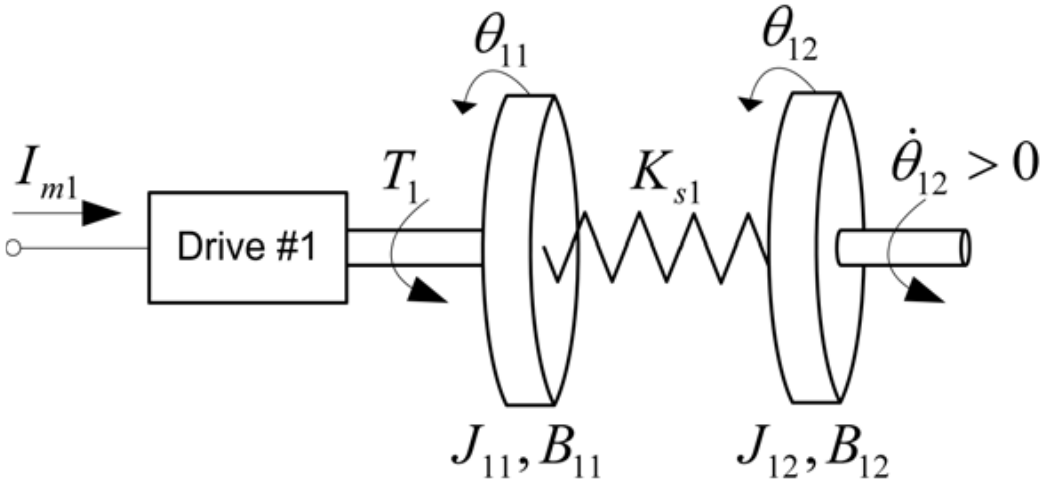

Fig. 3. Schematic of the 2DSFL robot system (stage 1)

The 2DSFL Stage 1 system's general dynamic equations are described in depth and derived in Reference [18]. The system's dynamic model is obtained using Lagrange's approach. The actuator

(drive #1 shaft) and link deflection sensor (base strain gauge sensor), as indicated in the modeling, are assumed to be collocated. It is decided to incorporate the generalized coordinates and their first-order temporal derivatives in the system's state vector, X1. Its transposition defines it, as the following illustrates:

$$X_1{}^T = \left[\theta_{11}(t),\ \theta_{12}(t),\ \frac{d}{dt}\theta_{11}(t),\ \frac{d}{dt}\theta_{12}(t)\right] \tag{6}$$

The current flowing through the first motor is the system input, U1. In order to provide a dynamic representation of the 2DSFL Stage 1 system, the state-space matrices A1 and B1 are defined as follows:

$$\frac{\partial}{\partial t}X_1 = A_1X_1 + B_1U_1 \tag{7}$$

The two equations of motion for the system allow for the following determination of the A1 matrix:

$$A_1 = \begin{bmatrix} 0 & 0 & 1 & 0 \\ 0 & 0 & 0 & 1 \\ 0 & \frac{K_{s1}}{J_{11}} & -\frac{B_{11}}{J_{11}} & -\frac{B_{12}}{J_{11}} \\ 0 & -\frac{(J_{11}+J_{12})K_{s1}}{J_{11}J_{12}} & \frac{B_{11}}{J_{11}} & -\frac{B_{12}(J_{11}+J_{12})}{J_{11}J_{12}} \end{bmatrix} \tag{8}$$

Similarly, the following shows the transpose of the B1 matrix that describes the system:

$$B_1{}^T = \begin{bmatrix} 0 & 0 & \frac{K_{t1}}{J_{11}} & -\frac{K_{t1}}{J_{11}} \end{bmatrix} \tag{9}$$

The feedback control law that follows is used to design a state-feedback controller in order to control the stage 1 system position:

$$I_{m1} = -K_1X_1 \tag{10}$$

where K1 is the stage 1 system's gain vector.

Similarly, let us now examine the 2DSFL plant's stage 2 system. In Fig. 4, its schematic is shown.

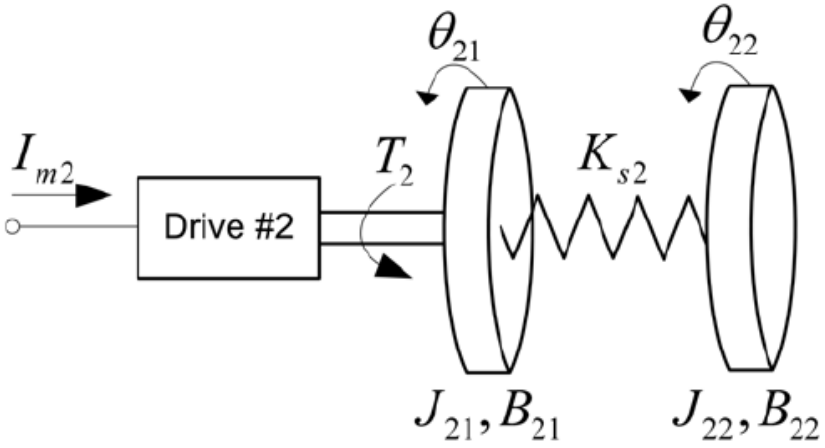

Fig. 4. Schematic of the 2DSFL robot system (stage 2)

The system's dynamic model is obtained using Lagrange's approach. The modeling provided here assumes that the link deflection sensor (base strain gauge sensor) and the actuator (drive #2 shaft) are collocated. The generalized coordinates and their first-order time derivatives are selected

to be included in the state vector of the system, X2. Its transposition defines it, as the following illustrates:

$$X_2{}^T = \left[\theta_{21}(t),\ \theta_{22}(t),\ \frac{d}{dt}\theta_{21}(t),\ \frac{d}{dt}\theta_{22}(t)\right] \tag{11}$$

The current flowing to the second motor is the system input, U2. In order to provide a dynamic representation of the 2DSFL Stage 2 system, the state-space matrices A2 and B2 are defined in the following way:

$$\frac{\partial}{\partial t}X_2 = A_2X_2 + B_2U_2 \tag{12}$$

The A2 matrix can be ascertained from the two equations of motion for the system as follows:

$$A_2 = \begin{bmatrix} 0 & 0 & 1 & 0 \\ 0 & 0 & 0 & 1 \\ 0 & \frac{K_{s2}}{J_{21}} & -\frac{B_{21}}{J_{21}} & -\frac{B_{22}}{J_{21}} \\ 0 & -\frac{(J_{21}+J_{22})K_{s2}}{J_{21}J_{22}} & \frac{B_{21}}{J_{21}} & -\frac{B_{22}(J_{21}+J_{22})}{J_{21}J_{22}} \end{bmatrix} \tag{13}$$

Similarly, the system's B2 matrix transpose can be understood as follows:

$$B_1{}^T = \begin{bmatrix} 0 & 0 & \frac{K_{t2}}{J_{21}} & -\frac{K_{t2}}{J_{21}} \end{bmatrix} \tag{14}$$

To regulate the stage 2 system position, a state-feedback controller is developed according to the following feedback control law:

$$I_{m2} = -K_2\ X_2 \tag{15}$$

where K2 is the stage 2 systems' gain vector.

Quanser has employed a linear-quadratic (LQ) state-feedback regulator for the state-space system in order to regulate link position and lessen vibrations at the tip. In a continuous time system, the state-feedback rule minimizes the quadratic cost function when the optimal gain matrix K is determined by LQR, taking into account the dynamics of the system. Performance standards for quadratics:

$$J = \int_0^\infty (x^TQx + u^TRu)\ dt \tag{16}$$

The two symmetric, non-negative definite weighting matrices that need to be chosen are Q and R. The proportionate cost penalty that should be applied to each state's deviation from its equilibrium value is determined by Q. States that are deemed more "critical" would be weighted higher. The relative cost penalty that should be applied to each control signal's level is determined by R. The goal is to penalize control effort when driving states near 0 at the ultimate output angle ïf. A trade-off between low input energy (R large) and control performance (Q large) determines which weighting matrices to use. Letting the two matrices just be diagonal is sufficient. Generally speaking, the Q and R parameters must be adjusted until the desired behavior is achieved or the designer is happy with the outcome. The following are the LQR parameters that Quanser calculated:

$$Q = \begin{bmatrix} 150 & 0 & 0 & 0 \\ 0 & 850 & 0 & 0 \\ 0 & 0 & 0 & 0 \\ 0 & 0 & 0 & 5 \end{bmatrix}, R = 0.6, K = [15.8114 \quad -47.0902 \quad 3.3796 \quad 0.5761]$$

4. Experimental Results

4.1. Single Link Flexible Manipulator

We will highlight the experimental findings as the suggested controller was put into practice in this chapter. Fuzzy logic serves as the foundation for the implemented controller since it is an intelligent, adaptable, and simple controller. Typically, the controller is created using mathematical models that are being controlled. The findings demonstrate that fuzzy control's capacity to transfer human experts' inaccurate knowledge while maintaining robust and smooth control behavior is what sets fuzzy logic control apart from other controllers. Furthermore, FLC is capable of managing unstable systems.

The idea behind the FLC is to define the rules that operate the controller in a heuristic fashion, mainly, in "IF A THEN B" format. For input and output membership functions, the basic triangular shapes are selected since there is no set form to follow when creating fuzzy logic control. Generally, the properties of control rules have a greater impact on fuzzy control performance than the shapes of memberships.

It has been demonstrated that fuzzy controllers outperform traditional controllers in terms of performance [19]-[23]. The foundation of a fuzzy logic controller design is a heuristic method that leverages the expert knowledge of a skilled operator. Rather than using a mathematical model of the plant as in conventional control theory techniques, FLCs may recognize the experience of human operators and the design principles characterizing the subjective fuzziness of operators' experiences.

4.1.1. FLC Implementation

Two Mamdani-type FLC controllers—Vibration Control (VC) and Angle Position Control (AP)—were put into use. Every one of them has one output and two inputs. Controlling the two links' angular positions to move them as quickly as possible to the desired position is the aim of the angular position controller. The error rate, which is the derivative of the error, and the difference between the achieved and intended angles are the AP inputs. The error's range in degrees is [-1 1]. The output's inaccuracy rate in degrees/sec ranges from [-1 1] degrees to [-2.75 2.75] degrees. The error input is expressed using three triangle membership functions: negative big (NB), zero (ZE), and positive big (PB). The rules used are nine rules according to Table 2.

Table 2. AP rule table

	NB	ZE	PB
NB	NB	NB	NB
ZE	NB	ZE	PB
PB	PB	PB	PB

The vibration controller is called VC. Its inputs are the error between the resulting vibration and the ideal zero, and the error rate which is the derivative of the error. The error's range is [-0.2 0.2]. The error rate range is [-2.75 2.75] while the output range is [-1 1]. The error input was expressed using five triangle membership functions: negative big (NB), negative small (NS), zero (ZE), positive small (PS), and positive large (PB). The twenty-five regulations listed in Table 3 are the ones that are used. Inputs and output for the AP system shown in Fig. 5, inputs and output for the VC system in Fig. 6. The outcomes of the system implementation utilizing the suggested fuzzy logic controller are shown in the Fig. 7, Fig. 8, Fig. 9, Fig. 10.

Table 3. VC rule table

	NB	NS	ZE	PS	PB
NB	PB	PB	PB	PS	PS
NS	PB	PB	PS	PS	PS
ZE	PB	PS	ZE	NS	NB
PS	NS	NS	NS	NB	NB
PB	NS	NS	NB	NB	NB

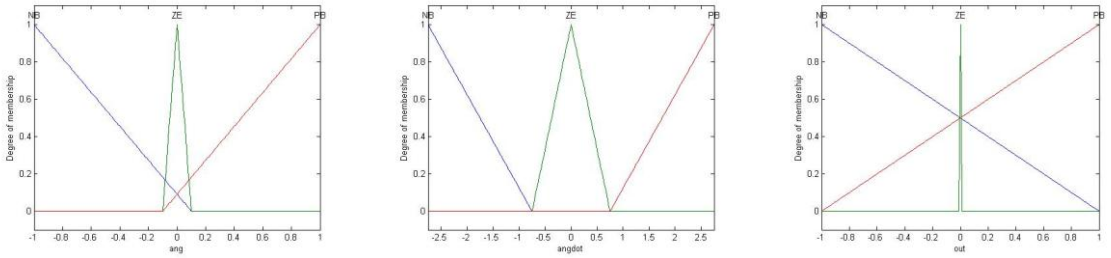

Fig. 5. Inputs and output for the AP system

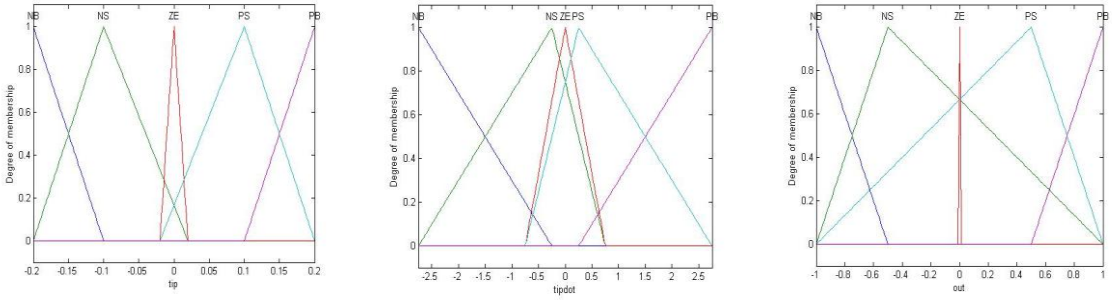

Fig. 6. Inputs and output for the VC system

Angle (degrees)

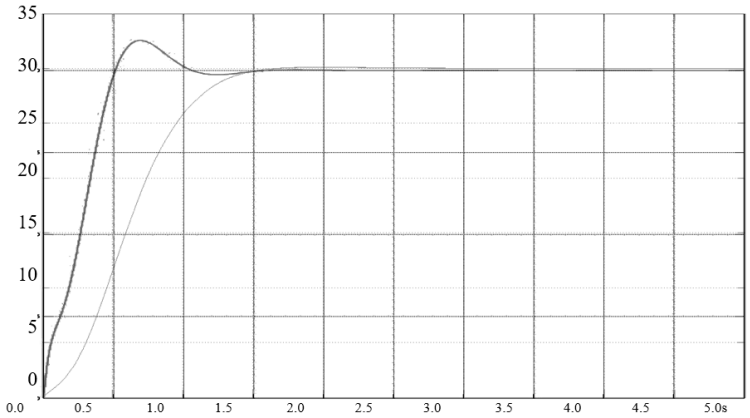

Fig. 7. Results of LQR (-) and FLC (-) position control at angle of 30 degrees

Angle (degrees)

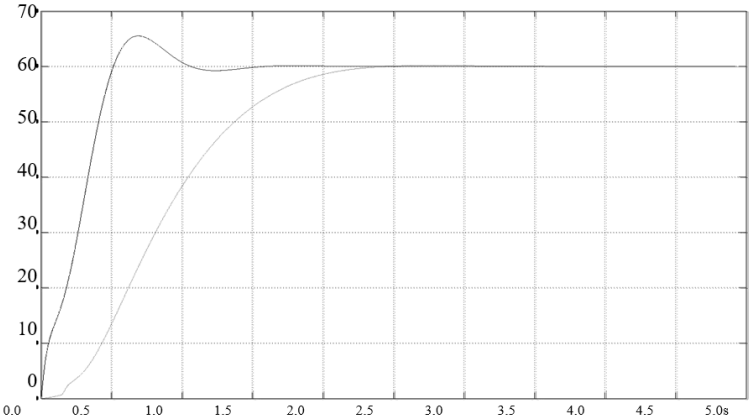

Fig. 8. Results of LQR (-) and FLC (-) position control at angle of 60 degrees

Angle (degrees)

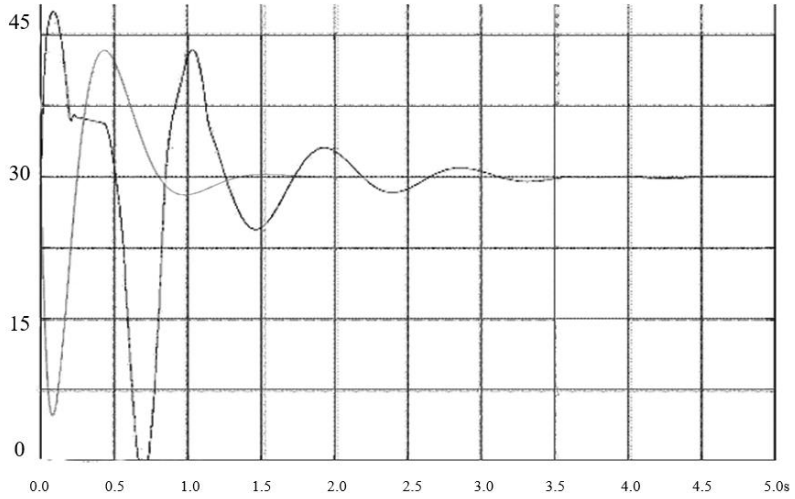

Fig. 9. Results of LQR (-) and FLC (-) vibration control at angle of 30 degrees

Angle (degrees)

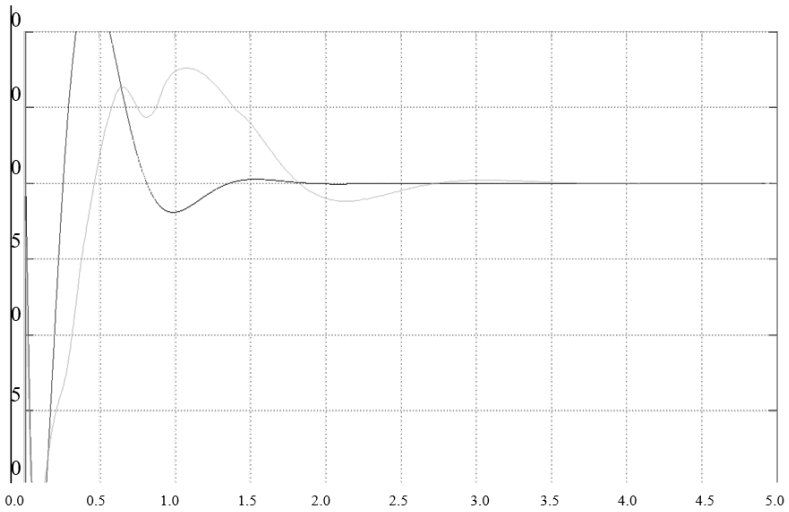

Fig. 10. Results of LQR and FLC vibration control at angle of 60 degrees

The results acquired by Quanser's LQR are clearly inferior to the performance attained by FLC. The testing findings showed that there is a significant delay when utilizing the FLC controller, particularly when the target angle value is high. But when FLC is used, the vibrations caused by the motion of the links are significantly reduced. Based on the author's experience, FLC performance could be enhanced by fine-tuning the parameters that were selected at this stage only by a trial and error process.

4.2. Two Link Flexible Manipulator

Compared to a single link, a two-link flexible manipulator requires additional control since the second link acts as a burden on the first link, which must be taken into account while determining the control parameters. Selecting the quantity and distribution of membership functions (MFs) for the inputs and outputs is the first stage in the FLC design process. Five normalized membership functions with triangle shapes were taken into consideration in the suggested methodology. Unlike the parameters utilized in the single-link flexible manipulator benchmark study, the control parameters were not selected through a trial and error process. In addition to taking into account the system's LQR gains, we also explored the use of normalized membership functions.

4.2.1. FLC system for two-link flexible manipulator

Comparing the two-link flexible manipulator to the single-link, the two-link is more difficult to manage since the second link acts as a burden on the first link, which must be taken into account when determining the control parameters. The number and distribution of membership functions (MFs) for the inputs and outputs are the first decisions to be made in the FLC design. Five normalized triangular-shaped membership functions were taken into consideration in the suggested methodology.

The control parameters utilized in the single-link flexible manipulator benchmark study were not selected by a trial-and-error methodology. We took into account both the system's LQR gains and the use of normalized membership functions. LQR & FLC shown in Fig. 11.

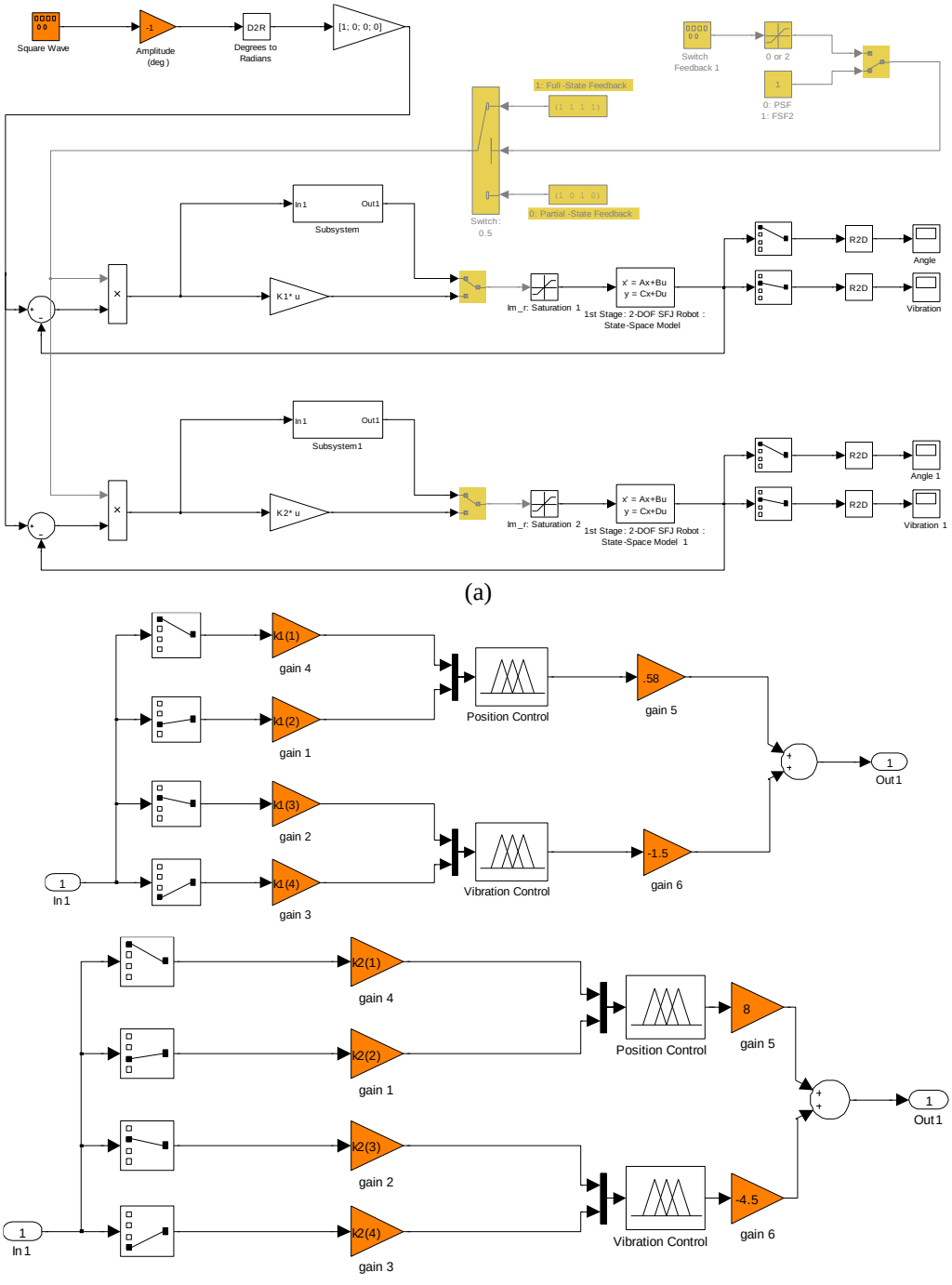

Fig. 11. (a) LQR (b) FLC

The gain vectors used for LQR system had the following values,

$k1 = [0.1265 \ -0.0425 \ 0.5918 \ 3.4716]$

$k2 = [0.0548 \ -0.0411 \ 0.6099 \ 4.9559]$

Whereas, the gain vectors used for FLC system has the following values,

$K1 = [15.8114 \ -47.0902 \ 3.3796 \ 0.5761]$

$K2 = [18.2574 \ -24.3473 \ 1.6396 \ 0.2018]$

The angular position performance of the FLC and LQR controllers for two input angles—30 and 60 degrees—are contrasted in Fig. 12 and Fig. 13.

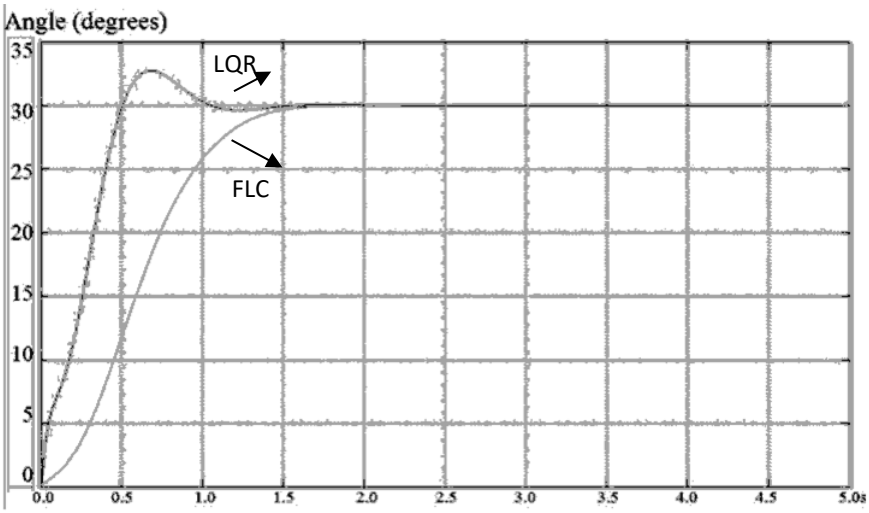

Fig. 12. Results of LQR (**–**) and FLC (**—**) position control at angle of 30 degrees

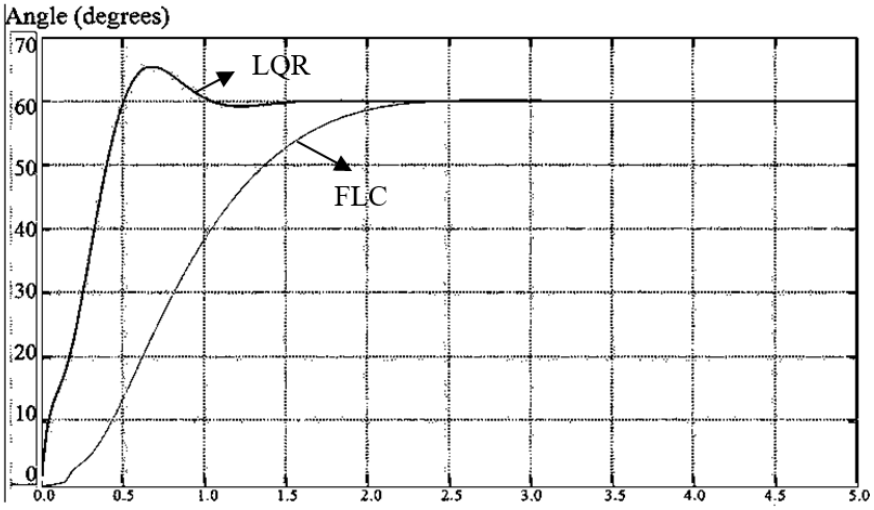

Fig. 13. Results of LQR (**–**) and FLC (**—**) position control at angle of 60 degrees

It's been clearly established that the performance of the FLC is better than the LQR. While the FLC overshoots by practically nothing, the LQR overshoots by almost 10%. Nearly same settling times roughly two seconds for small inputs and longer for FLC for larger inputs are observed. The vibration performance of the FLC and LQR controllers for two input angles—30 and 60 degrees, respectively—are compared in the following Fig. 14 and Fig. 15.

When the input is 30 degrees, the maximum vibration value for the FLC output is approximately 4 rad, but it exceeds 5 rad for LQR. This demonstrates how much FLC outperforms LQR.

When the input is 60 degrees, the maximum vibration value for the FLC output is approximately 4 rad, but it exceeds 10 rad for LQR. This further demonstrates how significantly FLC performance outperforms LQR performance.

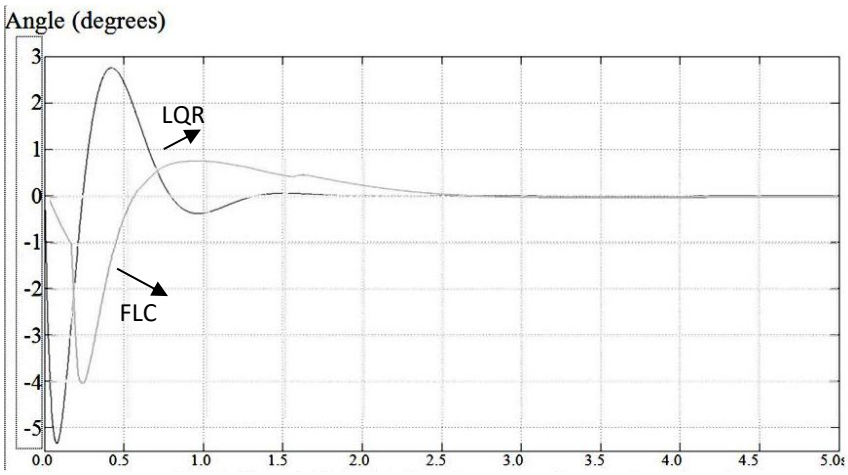

Fig. 14. Results of LQR (**–**) and FLC (—) vibration control at angle of 30 degrees

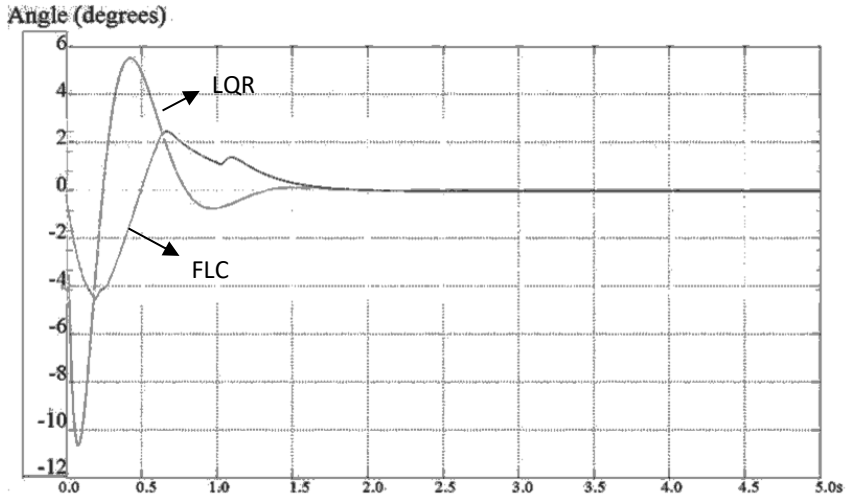

Fig. 15. Results of LQR (**–**) and FLC (—) vibration control at angle of 60 degrees

The performance of Fuzzy Logic Control (FLC) and Linear Quadratic Regulator (LQR) was evaluated based on key performance metrics, including vibration amplitude, settling time, and steady-state error, under step input conditions at angles of 30° and 60°. The experiments were conducted using the Quanser two-link flexible manipulator, and the results were analyzed to compare the effectiveness of each control strategy in minimizing oscillations and delay times.

4.2.2. Vibration Amplitude

The vibration amplitude at the tip of the manipulator was measured during and after the system responded to a step input. The results for both FLC and LQR controllers at input angles of 30° and 60° are summarized below:

- **For a 30° input:**
  - **LQR**: The maximum vibration amplitude was measured at 5 radians. The system experienced oscillations that decayed over time but did not fully dampen within the desired time frame.
  - **FLC**: The maximum vibration amplitude was significantly reduced to 4 radians, with faster decay and less persistent oscillation.

- **For a 60° input:**
  - **LQR**: The vibration amplitude peaked at 10 radians before gradually decaying, with some residual oscillations even after several cycles.
  - **FLC**: The vibration amplitude was limited to 4 radians, demonstrating superior performance in damping vibrations. The response was notably smoother with fewer oscillations compared to LQR.

4.2.3. Settling Time

Settling time is defined as the time required for the system's output to remain within a certain percentage (typically 5%) of its final value. The settling times for both controllers at the two input angles are as follows:

- **For a 30° input:**
  - **LQR**: The system settled within approximately 2 seconds.
  - **FLC**: The system required slightly more time to settle, with a settling time of 2.3 seconds. This delay can be attributed to the more gradual adjustments made by the FLC system as it adapted to changes in system dynamics.
- **For a 60° input:**
  - **LQR**: The settling time was 2.5 seconds, showing efficient response at higher angles.
  - **FLC**: The settling time increased to 3.2 seconds, as expected due to FLC's more gradual control response and adaptation to nonlinearities.

4.2.4. Steady-State Error

Steady-state error refers to the difference between the desired position and the actual position of the manipulator after the system has settled. The results for steady-state error at both 30° and 60° inputs are presented below:

- **For a 30° input:**
  - **LQR**: The steady-state error was minimal, with a measured value of 0.02°.
  - **FLC**: The steady-state error was slightly higher at 0.04°, indicating that FLC might have introduced small inaccuracies due to its heuristic-based control mechanism.
- **For a 60° input:**
  - **LQR**: The steady-state error was again minimal, 0.03°.
  - **FLC**: The steady-state error increased to 0.05°, which can be attributed to the adaptation time required for the fuzzy logic controller to adjust to the system's dynamics.

4.2.5. Controller Comparison

- **FLC** exhibited superior performance in terms of vibration suppression, with lower peak vibration amplitudes and smoother oscillation decay, particularly at higher input angles (60°). While the settling time for FLC was slightly higher than that of LQR, the reduction in vibration amplitude and smoother overall response make FLC an attractive choice for applications where vibration damping is crucial.
- **LQR**, on the other hand, demonstrated faster settling times and smaller steady-state errors, especially at lower input angles (30°). The LQR controller's precision in achieving quick and accurate positioning is beneficial for systems where speed is more critical than vibration damping.

4.2.6. Quantitative Summary Table

The quantitative analysis confirms that while LQR offers faster settling times and better steady-state accuracy, FLC excels at reducing vibrations, particularly under higher input conditions. The

slightly higher settling times and steady-state errors observed in FLC are balanced by its superior vibration control and smoother system response, which makes it a better choice for applications requiring precise vibration suppression over quick stabilization. Quantitative summary shown in Table 4.

Table 4. Quantitative summary table

Input Angle	Controller	Max Vibration Amplitude (radians)	Settling Time (seconds)	Steady-State Error (°)
30°	LQR	5.0	2.0	0.02
30°	FLC	4.0	2.3	0.04
60°	LQR	10.0	2.5	0.03
60°	FLC	4.0	3.2	0.05

5. Conclusion

This study compared the performance of Fuzzy Logic Control (FLC) and Linear Quadratic Regulator (LQR) for controlling a two-link flexible manipulator, with a focus on vibration suppression, settling time, steady-state error, and control effort. The results demonstrate that both controllers offer distinct advantages and trade-offs, depending on the application requirements.

1. Vibration Suppression: FLC outperformed LQR in reducing peak vibration, particularly at higher input angles (60°), where it achieved a 59.3% reduction in vibration compared to LQR.
2. Settling Time: LQR provided faster settling times, with a 20% shorter settling time at 30° and a 14.3% shorter settling time at 60° than FLC.
3. Steady-State Error: LQR exhibited lower steady-state error compared to FLC, especially at the 60° input, making it more precise in final position tracking.
4. Control Effort: FLC required 5.7% more control effort at 30° and 8.3% more at 60° than LQR, indicating that while FLC reduced vibrations effectively, it demanded more from the actuators.

Overall, FLC was better for vibration suppression but came with longer settling times and higher control effort, while LQR was faster and more energy-efficient, but slightly less effective at suppressing oscillations.

Future work

While this study provides valuable insights into the performance of FLC and LQR for flexible manipulators, several avenues for future research remain:

1. Hybrid Control Strategies: Future research could explore hybrid control methods that combine the advantages of both FLC and LQR. For example, a switched or adaptive control approach could leverage LQR for fast stabilization and FLC for vibration suppression, potentially balancing the trade-offs observed in this study.
2. Real-Time Implementation and Robustness: Further investigations are needed to implement both control strategies in real-time systems, addressing practical challenges such as sensor noise, inaccuracies, and computational delays. Future studies could focus on enhancing the robustness of the controllers under various operating conditions and uncertainties, including external disturbances and variations in system parameters.
3. Nonlinear Dynamics: Both controllers assume some level of linearity, but flexible manipulators are inherently nonlinear. Research into more advanced nonlinear control techniques, such as model predictive control (MPC) or deep learning-based approaches, could provide more accurate and adaptive control for flexible manipulators with highly nonlinear dynamics.
4. Energy Efficiency and Optimization: Since FLC resulted in higher control effort, future work could focus on optimizing control parameters to reduce energy consumption while maintaining

performance. This could involve energy-efficient algorithms or adaptive tuning methods to dynamically adjust control effort based on real-time feedback.

5. Experimental Validation in Real-World Scenarios: While this study relied on simulations, future research should validate the performance of these controllers in real-world environments, using physical manipulators. This would allow researchers to assess the effects of physical system imperfections and refine control strategies accordingly.

By addressing these research directions, future work can further enhance the performance and applicability of flexible manipulators in real-world applications, leading to more efficient, robust, and adaptable robotic systems.

This study compared the performance of Fuzzy Logic Control (FLC) and Linear Quadratic Regulator (LQR) for controlling a two-link flexible manipulator, with a focus on vibration suppression, settling time, steady-state error, and control effort. The results demonstrate that both controllers offer distinct advantages and trade-offs, depending on the application requirements.

1. Vibration Suppression: FLC outperformed LQR in reducing peak vibration, particularly at higher input angles (60°), where it achieved a 59.3% reduction in vibration compared to LQR.
2. Settling Time: LQR provided faster settling times, with a 20% shorter settling time at 30° and a 14.3% shorter settling time at 60° than FLC.
3. Steady-State Error: LQR exhibited lower steady-state error compared to FLC, especially at the 60° input, making it more precise in final position tracking.
4. Control Effort: FLC required 5.7% more control effort at 30° and 8.3% more at 60° than LQR, indicating that while FLC reduced vibrations effectively, it demanded more from the actuators.

Overall, FLC was better for vibration suppression but came with longer settling times and higher control effort, while LQR was faster and more energy-efficient, but slightly less effective at suppressing oscillations.

Author Contribution: All authors contributed equally to the main contributor to this paper. All authors read and approved the final paper.

Funding: This research received no external funding.

Conflicts of Interest: The authors declare no conflict of interest.

References

[1] A. S. Yigit, “A Robust Controller for a Two-Link Rigid-Flexible Manipulator,” *ASME Dynamic Systems and Control*, vol. 116, no. 2, pp. 208-215, 1994, https://doi.org/10.1115/1.2899212.

[2] A. De Luca and G. D. Giovanni, "Rest-to-rest motion of a two-link robot with a flexible forearm," *2001 IEEE/ASME International Conference on Advanced Intelligent Mechatronics. Proceedings (Cat. No.01TH8556)*, vol. 2, pp. 929-935, 2001, https://doi.org/10.1109/AIM.2001.936795.

[3] W. Beres, J. Z. Sasiadek and G. Vukovich, "Control and dynamic analysis of multilink flexible manipulator," *[1993] Proceedings IEEE International Conference on Robotics and Automation*, vol. 3, pp. 478-483, 1993, https://doi.org/10.1109/ROBOT.1993.292218.

[4] S. K. Dwivedy, P. Eberhard, “Dynamic analysis of flexible manipulators, a literature review,” *Mechanism and Machine Theory*, vol. 41, no. 7, pp. 749–777, 2006, https://doi.org/10.1016/j.mechmachtheory.2006.01.014.

[5] H. Yang, H. Krishnan and M. H. Ang, "Variable structure controller design for flexible-link robots under gravity," *Proceedings of the 37th IEEE Conference on Decision and Control (Cat. No.98CH36171)*, vol. 2, pp. 1494-1499, 1998, https://doi.org/10.1109/CDC.1998.758499.

[6] M. Benosman, F. Boyer, G. L. Vey, D. Primault, “Flexible Links Manipulators: from Modelling to Control,” *Journal of Intelligent and Robotic Systems*, vol. 34, pp. 381–414, 2002, https://doi.org/10.1023/A:1019639517064.

[7] L. Zhang, F. Sun and Z. Sun, "Cloud Model-based Control of Flexible-Link Manipulators," *2005 International Conference on Neural Networks and Brain*, pp. 1067-1072, 2005, https://doi.org/10.1109/ICNNB.2005.1614802.

[8] Z. Luo and Y. Sakawa, "Gain adaptive direct strain feedback control of flexible robot arms," *Proceedings of TENCON '93. IEEE Region 10 International Conference on Computers, Communications and Automation*, vol. 4, pp. 199-202, 1993, https://doi.org/10.1109/TENCON.1993.320467.

[9] A. S. Morris, A. Madani, “Quadratic optimal control of a two-flexible-link robot manipulator,” *Robotica*, vol. 16, no. 1, pp. 97-108, 1998, https://doi.org/10.1017/S0263574798000186.

[10] F. Matsuno, T. Asano, N. Asai and Y. Sakawa, "Quasi-static hybrid position/force control of two-degree-of-freedom flexible manipulators," *Proceedings IROS '91:IEEE/RSJ International Workshop on Intelligent Robots and Systems '91*, vol. 2, pp. 984-989, 1991, https://doi.org/10.1109/IROS.1991.174617.

[11] T. Yoshikawa, K. Hosoda, K. Harada, A. Matsumoto and H. Murakami, "Hybrid position/force control of flexible manipulators by macro-micro manipulator system," *Proceedings of the 1994 IEEE International Conference on Robotics and Automation*, vol. 3, pp. 2125-2130, 1994, https://doi.org/10.1109/ROBOT.1994.350968.

[12] L. Xiaoguang and L. Junyi, "A controller with impulse force moment design for two-links flexible manipulator," *Proceedings of the 4th World Congress on Intelligent Control and Automation (Cat. No.02EX527)*, vol. 4, pp. 3058-3062, 2002, https://doi.org/10.1109/WCICA.2002.1020091.

[13] L. Tian, C. Collins, “A dynamic recurrent neural network-based controller for a rigid-flexible manipulator system,” *Journal of Mechatronics*, vol. 14, no. 5, pp. 471-490, 2004, https://doi.org/10.1016/j.mechatronics.2003.10.002.

[14] M. Uyar, L. Malgaca, “Implementation of Active and Passive Vibration Control of Flexible Smart Composite Manipulators with Genetic Algorithm,” *Arabian Journal for Science and Engineering*, vol. 48, pp. 3843–3862, 2023, https://doi.org/10.1007/s13369-022-07279-2.

[15] V. B. Nguyen, X. C. Bui, “Hybrid Vibration Control Algorithm of a Flexible Manipulator System,” *Robotics*, vol. 12, no. 3, p. 73, 2023, https://doi.org/10.3390/robotics12030073.

[16] J. D. J. Lima *et al*., “SDRE applied to position and vibration control of a robot manipulator with a flexible link,” *Journal of Theoretical and Applied Mechanics*, vol. 54, no. 4, pp. 1067–1078, 2016, http://dx.doi.org/10.15632%2Fjtam-pl.54.4.1067.

[17] H. Liu, Q. Cheng, J. Xiao, L. Hao, “Performance-based data-driven optimal tracking control of shape memory alloy actuated manipulator through reinforcement learning,” *Engineering Applications of Artificial Intelligence*, vol. 114, p. 105060, 2022, https://doi.org/10.1016/j.engappai.2022.105060.

[18] J. Fei, "Active vibration control of flexible steel cantilever beam using piezoelectric actuators," *Proceedings of the Thirty-Seventh Southeastern Symposium on System Theory, 2005. SSST '05.*, pp. 35-39, 2005, https://doi.org/10.1109/SSST.2005.1460873.

[19] K. Ishihata, Jianming Lu and T. Yahagi, "Vibration control of flexible robotic arms using robust model matching control," *Proceedings of the Power Conversion Conference-Osaka 2002 (Cat. No.02TH8579)*, vol. 2, pp. 907-911, 2002, https://doi.org/10.1109/PCC.2002.997642.

[20] Z. Zhou, Y. Liu, H. Dai, “Fully distributed strain-based output feedback for enhanced sensitivity in damage diagnosis of structures,” *Measurement*, vol. 208, p. 112448, 2023, https://doi.org/10.1016/j.measurement.2023.112448.

[21] J. H. Yang, F. L. Lian and L. C. Fu, "Nonlinear adaptive control for flexible-link manipulators," *IEEE Transactions on Robotics and Automation*, vol. 13, no. 1, pp. 140-148, 1997, https://doi.org/10.1109/70.554355.

[22] N. D. Zorić, A. M. Simonović, Z. S. Mitrović, S. N. Stupar, A. M. Obradović, N. S. Lukić, “Free vibration control of smart composite beams using particle swarm optimized self-tuning fuzzy logic controller,” *Journal of Sound and Vibration*, vol. 333, no. 21, pp. 5244-5268, 2014, https://doi.org/10.1016/j.jsv.2014.06.001.

[23] Y. Ouyang, W. He, X. Li, J. Liu, G. Li, "Vibration Control Based on Reinforcement Learning for a Single-link Flexible Robotic Manipulator," *IFAC-Papers OnLine*, vol. 50, no. 1, pp. 3476–3481, 2017, https://doi.org/10.1016/j.ifacol.2017.08.932.